

Correlation between α -synuclein and fatty acid composition in jejunum of rotenone-treated mice is dependent on acyl chain length

Dominika Hajduchova¹, Roman Holic², Peter Gajdos³, Milan Certik³, Erika Halasova⁴, Renata Pecova¹ and Michal Pokusa⁴ 

¹ Department of Pathological Physiology, Jessenius Faculty of Medicine in Martin, Comenius University in Bratislava, Martin, Slovakia

² Institute of Animal Biochemistry and Genetics, Centre of Biosciences, Slovak Academy of Sciences, Bratislava, Slovakia

³ Institute of Biotechnology, Faculty of Chemical and Food Technology, Slovak University of Technology, Bratislava, Slovakia

⁴ Biomedical Center Martin, Jessenius Faculty of Medicine in Martin, Comenius University in Bratislava, Martin, Slovakia

Abstract. Events associated with the progression of Parkinson's disease (PD) are closely related to biomembrane dysfunction. The specific role of membrane composition in the conformational stability of alpha synuclein (α S) has already been well documented. Administration of rotenone is one of the best strategies to initiate PD phenotype in animal models. In the present study, daily exposure (14 weeks) of orally administered rotenone (10 mg/kg) was employed in a mouse model. The mitochondrial complex I inhibition resulted in elevated level of α S in whole tissue homogenate of mouse jejunum. In addition, we identified a strong intra-individual correlation between α S level and the specific esterified fatty acids. The observed correlation depends mainly on the acyl chain length. Based on the obtained results, it is suggested that there is a high potential to manipulate fatty acid homeostasis in modulating α S based pathogenesis of PD, at least in experimental conditions.

Key words: Parkinson's disease — Alpha synuclein — Gastrointestinal tract — Fatty acids — Mitochondrial complex I inhibition

Introduction

Parkinson's disease (PD) is a highly prevalent neurodegenerative disease characterized by the motor symptoms that worsen with advancing age (Xia and Mao 2012; Wang et al. 2013). The manifestation of PD is mainly associated with the degeneration of progressive dopaminergic neurons in *substantia nigra pars compacta*. Moreover, several other common signs of the disease can be identified on the subcellular level. Accordingly, PD is considered to be a classical proteinopathy. High PD prevalence is primarily associated with incorrect folding of α -synuclein (α S) protein into fibrillar

aggregates that later give rise to the formation of Lewy bodies (LBs) (Braak et al. 2003; Fanning et al. 2020). In relation to intracellular lipid turnover, the dysfunction of membrane homeostasis, including vesicular transport or mitochondrial membrane dynamics, has been observed in PD pathology (Panicker et al. 2021). Moreover, α S that disrupts the integrity of cell membranes is assumed to play an important role in these pathological processes (Varkey et al. 2010). Also, α S overexpression in cells is considered as the platform for Golgi apparatus fragmentation (Fujita et al. 2006), mitochondrial degradation (Martin et al. 2006), and the damage of lysosomes (Meredith et al. 2002), endoplasmic reticulum, and nuclear membranes (Stichel et al. 2007). In addition, lipids, which represent main component of LB, are considered to be derived from degraded membrane organelles (Gai et al. 2000; Varkey et al. 2010). So far, the above-described PD-associated alterations have been considered as the consequences of the

Correspondence to: Michal Pokusa, Biomedical Center Martin, Jessenius Faculty of Medicine in Martin, Comenius University in Bratislava, 036 01 Martin, Slovakia
E-mail: michal.pokusa@uniba.sk

existing pathology rather than its cause. However, the results of several recent studies highlight the role of primary lipid dysfunction in the α S dyshomeostasis, which could result in the reclassification of PD from exclusive proteinopathy to lipidopathy (Fanning et al. 2020).

Disorders of α S-membrane interactions are currently considered as potential triggers of α S toxic oligomerization (Burré et al. 2015; Galvagnion et al. 2015). Thus, the specific nature of fatty acids in biomembranes may determine the initiation of pathological events associated with α S dyshomeostasis (Sharon et al. 2003a). The contribution of saturated fatty acids representatives like palmitic acid (PA, C16:0), stearic acid (SA, C18:0), and arachidic acid (AA, C20:0) is particularly interesting. Significantly elevated levels of PA and SA have been reported in plasma samples in experimental rat model of PD, which, in addition, correlated with the tests indicating motor dysfunction (Shah et al. 2019). In addition, a strong physical interaction of α S with SA has been observed (Ramakrishnan et al. 2003). In relation to the impact of PA on α S levels, a diet enriched with PA was found to increase α S levels in the brain of a mouse PD model (Schommer et al. 2018). Another study evaluating α S-membrane interactions revealed that stress in rat primary neurons caused by α S mutations of familial PD can be alleviated by increasing concentrations of SA, PA, or myristic acid (MA, C14:0) (Tripathi et al. 2022). Moreover, the treatment of mesencephalic neurons with saturated fatty acids, such as SA or AA, resulted in decreased levels of oligomeric α S (Alecú and Bennett 2019; Sharon et al. 2003a; Lücke et al. 2006).

In the terms of neurotoxicity that leads to high excesses of α S monomers, the accumulation of oleic acid (OA, C18:1 Δ^9) represents one of the best documented mono-unsaturated acid. Indeed, α S monomers are pro-aggregation precursors, which could be easily transformed into oligomers and fibrils as a basis for later formation of aggregates and LBs. In contrast, the reduction of SA conversion into OA simultaneously increased physiological α S multimerization into tetramers (Fanning et al. 2019; Imberdis et al. 2019). As demonstrated in cell and animal models, OA-producing stearoyl-CoA desaturase (SCD) inhibitors are effective in preventing α S cytotoxicity and protein inclusion. The precise mechanism is again defined by the preservation of the tetrameric form of α S by its binding to saturated lipids (Vincent et al. 2018; Fanning et al. 2019).

Increased α S oligomerization has also been observed in the presence of higher concentrations of several polyunsaturated fatty acids (PUFAs) (Perrin et al. 2001). The treatment of mesencephalic neuronal cells with α -linolenic acid (C18:3 $\Delta^{9,12,15}$) and eicosapentaenoic acid (C20:5 $\Delta^{5,8,11,14,17}$) has been observed to result in a dramatic increase of soluble α S oligomers (Sharon et al. 2003a; Lücke et al. 2006; Alecú and Bennett 2019). Docosahexaenoic acid (DHA, C22:6 $\Delta^{4,7,10,13,16,19}$) and, to a lesser extent, arachidonic acid

(ARA, C20:4 $\Delta^{5,8,11,14}$) are also able to induce α S oligomerization (Yakunin et al. 2012; Alza et al. 2019). In the cytoplasm of dopaminergic neuronal cells overexpressing α S, an intense α S oligomers formation was also observed after PUFA exposure. The presence of described oligomers led to the formation of protein inclusions similar to LBs, which subsequently initiated the formation of protein inclusions similar to LBs (Assayag et al. 2007). Regarding protein inclusions, the formation of oligomeric or fibrillar α S conformations in the presence of DHA have been found to depend on the protein to PUFA ratio. An aggregation into fibrils is promoted by molar ratios higher than 1:10. Besides, DHA seems to stimulate α S conformational changes in favour of the disappearance of physiological α -helical structure (Fecchio et al. 2018; Alza et al. 2019). DHA is also able to modulate the depth of α S insertion into the membrane, the structure and orientation of this protein within the membrane as well as membrane structure (Manna and Murarka 2021). Notably, an increase in free DHA levels has been observed in the cytosolic brain fractions of patients with PD and LBs dementia (Sharon et al. 2003b). ARA has a specific position among PUFAs. Despite the stimulation of the formation of α S oligomers, ARA is the only of the mentioned fatty acids that also promotes the maintenance of their α -helical structure, which is resistant to the formation of longer fibrils. In addition, these oligomers can be easily degraded by 26S proteasomes that prevent neuronal damage and reduce microglial activation (Iljina et al. 2016; Xylaki et al. 2020).

The inhibition of mitochondrial electron chain complex I, which can be achieved using rotenone, represents one of the platforms for α S overexpression in experimental *in vivo* and *in vitro* PD models (Giráldez-Pérez et al. 2014; Pokusa et al. 2021). In comparison to genetic or other toxic models of PD, the rotenone model is widely used especially due to the capability to recapitulate wide spectrum of pathological signs of PD (Shimohama et al. 2003). Laboratory *in vivo* studies with rotenone have repeatedly shown that it induces the loss of dopaminergic cells in *substantia nigra* as well as α S aggregation in affected cells (Innos and Hickey 2021). Most mice or rat models use system administration of toxin into bloodstream as well as straight stereotaxical injection into specific sites of central nervous system like *substantia nigra pars compacta* (Cannon et al. 2009; Xiong et al. 2009; Inden et al. 2011). Due to the neurodegenerative character of the disease, most toxic models are focused on the analysis of changes that occur in the central nervous system. After the accumulation of data about the presence of non-neuronal origin of certain proportion of PD cases, new designs of disease modelling were established continuously. Following the description of early pathological processes occurring in gastrointestinal tract (GIT), which were documented several years before central pathology establishment, one type of relatively new and well accepted toxic model based on

rotenone oral administration have been established. Several studies show that the toxin administration of 5–10 mg/kg by gastric tube gives rise to several documented hallmarks of PD, starting with the accumulation of α S in the GIT but also the spread of α S aggregates in the peripheral and central nervous system of mice (Pan-Montojo et al. 2010; Tasselli et al. 2013).

Most of the mentioned studies monitoring the interaction of α S with lipids use clinical samples or experimental models based on a different principle than the use of respiratory chain toxins. However, except the genetic predisposition, the environmental form of the disease is characterized as a similarly large group predominantly caused by various mitochondrial toxins (Fahn and Sulzer 2004). Changes in fatty acid metabolism are studied in these models mainly with the relevance to modulated energy metabolism (Worth et al. 2014). Animal models characterized by oral administration of rotenone can be defined as one of the most reliable models, which mimic the environmental cause of PD with the onset in the digestive system. Therefore, in this work, we focus on a possible correlation of changes in the composition of fatty acids with markers reflecting neurodegeneration in the digestive tract in above-mentioned animal model.

Material and Methods

Cell study

In *in vitro* experiments, commercial human neuroblastoma SH-SY5Y cell line was used. Cells were maintained and cultured in DMEM-F12 medium with 10% FBS, passaged after reaching 90% confluence. For the experimental use, cultures were held up to 80% confluence and up to 8th passage. In this study, a standard surface treated T75 culture flasks for adherent cultures was used for the cultivation of cells. Rotenone solution in DMSO was used in final concentration of 10 nM for 24 h. The stock solution was prepared as 1000× concentrate to minimize DMSO addition to cell culture. Three biological replicates were performed in control and rotenone influence conditions.

Animal study

The use of male C57BL/6J mice (Velaz, Czechia) with a body weight of 24–26 g was approved by the Slovak National Veterinary and Food Authority by decision number 1360/2020-220. Animals were kept in groups of 6 in transparent plastic cages with sawdust used as bedding at 23°C and 12/12 h dark/light cycles. Food and water were available *ad libitum*. Rotenone was administered orally in a dose of 10 mg/kg of bodyweight. Toxin was re-suspended in vehicle based on deionized water containing 1% chlorophorm

and 1% carboxymethylcellulose. For re-suspending 10 mg of rotenone, 5 ml of vehicle solution was used. Animals with a body weight of 30 g were administered 150 μ l of rotenone/vehiculum from Monday to Friday at 9 am. The control group of animals ($n = 6$) was held in the experiment for 12 weeks. The experimental group of animals ($n = 6$) was treated with rotenone for 14 weeks. For the purpose of samples collection, animals were exsanguinated in deep chloralhydrate anesthesia. The proximal portion of jejunum was collected as two parallel samples of ca 40–100 mg for the purpose of protein as well as lipid extraction. Excised tissue was processed in order to avoid the distortion of results by surrounding visceral fat and fibrous tissue. Cleaned jejunal samples were finally washed in PBS solution and stored in -80°C for the further procedure.

ELISA analysis

The measurement of two biomarkers in the intestinal tissue was performed by commercial ELISA kits for murine α S (SEB222Mu, Cloud-clone corp., USA) and for glucose regulated protein 78 (GRP78) (CSB-E17690M-96, Cusabio, Netherlands) according to the manufacturer's protocol. Markers were measured in tissue homogenate in T-PER buffer (78510, Thermo Fisher, USA) enriched with protease inhibitors (Protease mini, Thermo Fisher, USA) prepared by rotary homogenizer on ice. Tissue of 50 mg was homogenized in 500 μ l of homogenization buffer. After homogenization, homogenates were spun at $400 \times g$ and 4°C for 5 min. Supernatant was stored at -20°C until ELISA analysis was performed. Aliquots of supernatant were used to determine protein concentration by BCA assay (BCA kit, Thermo Fisher, USA). In order to use 50 μ g of extracted proteins in ELISA measurements, protein concentration of samples was adjusted by T-PER.

Western blot analysis

The evaluation of beta III tubulin (BIIIT) in tissue homogenate was performed by semiquantitative immunodetection of glycine-based PAGE separated samples blotted on PVDF membrane. Prepared homogenates (as described above) were boiled at 95°C for 5 min with LDL sample buffer and 2% mercaptoethanol. Then, 20 μ g of proteins/each sample were applied on 4–10% acrylamide/bisacrylamide (29:1) gel and Tris/glycine PAGE was performed at 300 V for protein separation. Proteins were blotted on PVDF membrane by semi-dry transfer at 25 V for 1 h. PVDF membrane was blocked with 2.5% BSA in TBS Tween-20 solution. Membrane was incubated overnight at 4°C with primary antibodies (mAb4466S, Cell signalling, USA) diluted 1:1000 by 2.5% BSA in TBS Tween-20. After washing the membrane for 3×10 min in TBS Tween-20, secondary antibodies bounded

with horseradish peroxidase (G-21040, Thermo Fisher, USA) diluted 1:10000 in TBS Tween-20 was added to membrane for 1 h at 20°C. The detection of luminescence signal after washing for 5×5 min was performed after one minute incubation with luminescence substrate (GE healthcare, USA). ImageJ software was used for the quantification of the signal.

Lipid extraction and transesterification of fatty acids

Lipid extraction from frozen tissue samples was performed according to Bligh and Dyer (1959). The initial volume of methanol was set up according to the weight of sample to sustain the ratio 200 µl of methanol to 100 mg of tissue. Samples were prepared on ice with the use of a rotary homogenizer. After lipid extraction, the methylation of esterified fatty acids was performed as described by Garaiova et al. (2017) with minor modifications. Aliquots (100 µl) of lipid extract in chlorophorm/methanol (2:1) were dried under a stream of nitrogen gas and transmethylated with 333 µl of 5% sodium methoxide in methanol at 30°C for 30 min. After incubation, 67 µl of internal standard (methyl heptadecanoate Sigma-Aldrich, USA, 5 mg/100 ml in hexane) was added into the sample. To stop the reaction, 500 µl of 0.9% NaCl was added and fatty acid methylesters (FAME) were extracted with 267 µl of hexane. The mixture was vortexed, centrifuged at 3000 × *g* for 5 min and the upper hexane phase containing FAMES was transferred to a glass vial. The rest of the sample was re-extracted with 300 µl of hexane, the upper hexane phase was then combined with the FAMES in the glass vial, and samples were stored at –20°C until gas chromatography (GC) analysis was performed.

For the purpose of lipid extraction from cell culture, SH-SY5Y cells were cultivated as described above. Cells were trypsinized and washed two times with ice cold PBS. An aliquot of 1×10^7 cells was transferred into a new tube, centrifuged, and re-suspended in 100 µl of ice-cold deionized water. Lipids were extracted according to Bligh and Dyer (1959) protocol with initial 300 µl of methanol added to the cell suspension. The lipid homogenate was dried under a stream of nitrogen gas and transmethylated by the protocol described above to obtain FAMES. Analysis of FAMES was carried out by the injection of 1 µl aliquot to a GC apparatus.

GC analysis

FAMES were analysed by GC-6890 N (Agilent Technologies, USA) and separated on a capillary DB-23 column (50%-cyanopropyl-methylpolysiloxane, a length of 60 m, a diameter of 0.25 mm, analysis conditions were as follows: carrier gas – hydrogen, inlet (230°C; hydrogen flow: 37 ml/min; split – 10:1), FID detector (250°C, hydrogen flow: 40 ml/min, air flow: 450 ml/min), gradient (150°C – 0 min; 150–170°C – 5.0°C/min; 170–220°C – 6.0°C/min; 220°C –

6 min; 220–230°C – 6°C/min; 230°C – 1 min; 230–240°C – 30°C/min; 240°C – 6 min). Chromatograms were analysed with Agilent Open LAB CDS software. Individual FAMES were identified by comparison with the authentic standards of the C4–C24 FAME mixture (Supelco, USA). Quantification of individual fatty acid was performed using the methyl heptadecanoate internal standard.

Statistics

The statistical evaluation was performed using Jamovi software. Student's *t*-test was used for the comparison of changes in level of markers and fatty acids between control ($n = 6$) and experimental ($n = 6$) group of animals as well as in the case of biological replicates of control and treated cell culture of SH-SY5Y. A *p*-value less than 0.05 was considered to be statistically significant. The strength of significance was expressed in the graphs by asterisks: *p*-value ranging 0.05–0.01 corresponded to *, 0.01–0.001 corresponded to **, and *p*-value lower than 0.001 was expressed as ***. The level of association between intra-individually measured values was assessed by Pearson's coefficient (*r*) in experimental ($n = 6$) and control ($n = 6$) groups of animals separately. The correlation was evaluated as very low when $0 < r < \pm 0.19$, low when $\pm 0.2 < r < \pm 0.39$, moderate when $\pm 0.4 < r < \pm 0.59$, strong $\pm 0.6 < r < \pm 0.79$, and as very strong when $\pm 0.8 < r < \pm 1$.

Results

The purpose of this study was to investigate the association between fatty acids and markers relevant for neurodegeneration in early stages of PD. Our methodological approach included the inhibition of the mitochondrial complex I by rotenone as a well-recognized tool for the induction of neurodegeneration in different experimental model systems. In the first phase of the study, the data was obtained from the study on SH-SY5Y. Overall, the rotenone treatment for 24 h led to significant changes of several fatty acids. Specifically, fatty acids that were upregulated belonged to very long-chain ($C_{22} \leq$) as well as long-chain fatty acids (C_{14} – C_{20}) group (Table 1). The tendency of increase was observed in 9 fatty acids; however, the statistical analysis revealed the significant change in stearic acid ($C_{18:0}$), γ -linolenic acid ($C_{18:3\Delta^{6,9,12}}$), eicosanoic acid ($C_{20:0}$), docosanoic acid ($C_{22:0}$), and docosadienoic acid ($C_{22:2\Delta^{13,16}}$). On the contrary, rotenone treatment more likely caused a decrease of fatty acids only in a group of shorter (long-chain) fatty acids. The tendency of decrease was observed in 5 fatty acids. Statistical significance was confirmed namely in the case of palmitic acid ($C_{16:0}$); oleic acid ($C_{18:1\Delta^9}$), cis-vaccenic acid ($C_{18:1\Delta^{11}}$), and eicosadienoic acid ($C_{20:2\Delta^{11,14}}$) (Table 1).

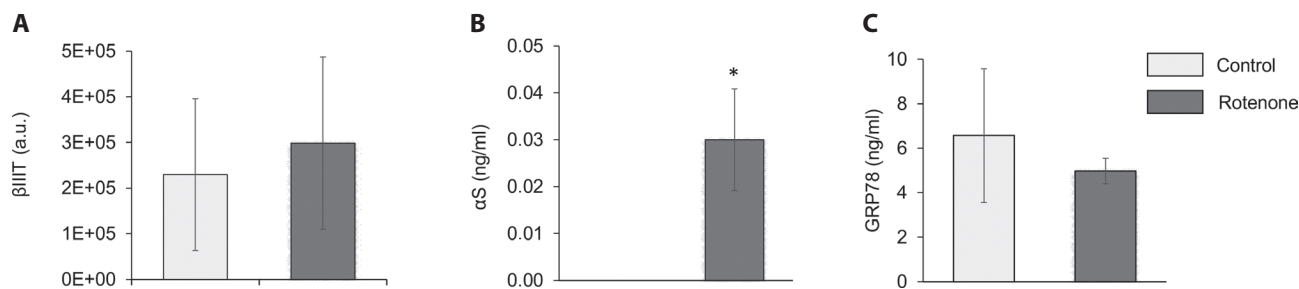


Figure 1. Graphic illustration of measured markers in control group treated with vehiculum and rotenone-treated group of animals. **A.** Relative levels of beta III tubuline (β IIIT) was determined by Western blot analysis. Alpha synuclein (α S, **B**) and glucose-regulated protein 78 (GRP78, **C**) concentrations were determined by ELISA test. Whole tissue homogenate from jejunum was used for all analysis. Values are represented as means \pm SEM in each group ($n = 6$ animals). Statistical significance was evaluated by Student's t -test as follows: α S ($t = -2.76$, $df = 10$, $p = 0.02$), β IIIT ($t = -0.674$, $df = 10$, $p = 0.516$) and GRP78 ($t = -0.524$, $df = 10$, $p = 0.612$). Significant change of rotenone-treated group is marked by the asterisk ($* p < 0.05$).

In animal experiment, chronic oral treatment by rotenone was performed in order to establish the initial stages of neurodegeneration localized predominantly in gastrointestinal tract. For the confirmation of pathology establishment, three selected markers were evaluated by ELISA measurement in whole tissue homogenate of jejunum. No significant change was observed in the case of β IIIT and GRP78 (Fig. 1). In control samples, we did not observe any detectable level of α S. In the rotenone-treated group of animals, expression of α S was confirmed in 4 samples.

Small intestine sample of each animal was processed for the analysis of esterified fatty acids. Among 17 fatty acids detected in this type of tissue, we did not reveal any significant changes between quantity comparing experimental and control group of animals (data not presented). The variety of data obtained from each individual animal was suitable for intra-individual comparison. The correlation analysis of fatty acids and selected biomarkers (Fig. 2) revealed an interesting pattern in rotenone treated group of animals. According to Pearson's coefficient, a strong correlation could be seen between α S and fatty acids in rotenone-treated group of animals. Moreover, an intermediate correlation between β IIIT and measured fatty acids has appeared in rotenone-treated group as well. The pattern of association of both factors (α S and β IIIT) with a specific type of fatty acid appears to be opposite (Fig. 2). GRP 78 exhibits the lowest association with fatty acid compound while rotenone treatment has probably no effect on this pattern. Interesting fact is evident after dividing fatty acids compilation according to their chain length. Specifically, α S is almost exclusively negatively associated with fatty acids ranging from C14 to C18 while its positive correlation is evident with fatty acids C20 and higher. The opposite pattern could be found in the case of β IIIT and GRP78 in which the tendency of positive correlation is observed in C14–C18 group of identified fatty acids. Detailed insight

into Figure 2 and 3 indicates an importance of stearic acid (C18:0), which is the only fatty acid reacting in the opposite way than C14–C18 long-chain fatty acids. Similar situation was observed in the group of $C_{20} \leq$ fatty acids with gondoic acid (C20:1 Δ^{11}). The deviated behaviour of these two fatty acids was confirmed also by the correlation

Table 1. Effect of rotenone on fatty acids of cell culture SH-SY5Y

Fatty acid	p -value	t -value	Significance	Up/down-regulated
<i>Long-chain</i>				
C14:0	0.143	-1.818	No	Up
C16:0	0.01	4.593	**	Down
C16:1 Δ^7	0.392	0.959	No	Down
C16:1 Δ^9	0.862	0.185	No	Down
C18:0	0.031	-3.263	*	Up
C18:1 Δ^9	0.002	6.966	**	Down
C18:1 Δ^{11}	0.023	3.609	*	Down
C18:3 $\Delta^{6,9,12}$	0.011	-4.437	*	Up
C20:0	0.024	-3.562	*	Up
C20:2 $\Delta^{11,14}$	0.022	3.651	*	Down
C20:4 $\Delta^{5,8,11,14}$	0.117	-1.994	No	Up
<i>Very long-chain</i>				
C22:0	0.023	-3.574	*	Up
C22:2 $\Delta^{13,16}$	0.006	-5.271	**	Up
C22:6 $\Delta^{4,7,10,13,16,19}$	0.303	-1.18	No	Up
C24:0	0.063	-2.556	No	Up

Effect of rotenone is evaluated by comparison of cell culture exposed to 10 μ M rotenone for 24 h to control cells. Significance of changes is determined by Student's t -test performed on 3 biological replicates of both control and rotenone treated cells ($df = 4$). * $p < 0.05$, ** $p < 0.01$.

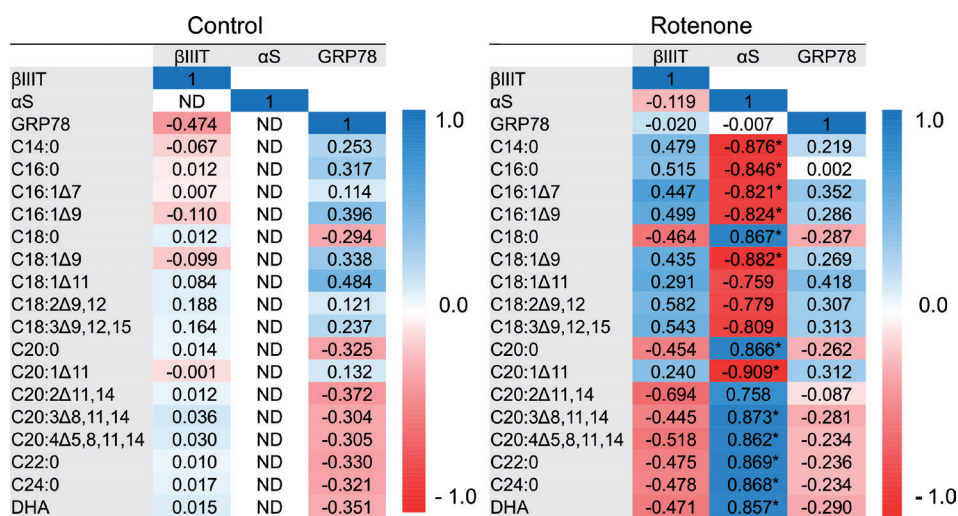


Figure 2. Comparison of correlation matrix created on data obtained from control ($n = 6$) vs. rotenone-treated ($n = 6$) animals in the study. Association levels were established intraindividually among specific fatty acids vs. alpha synuclein (α S), beta III tubuline (β IIIT) and chaperone protein GRP78. Intensity of blue/red colour reflects strength of Pearson's coefficient. Positive correlation is expressed by blue shade, while red colour is relevant for negative manner of association between compared

molecules. Correlation of α S was evaluated as non defined (ND) because of undetectable concentrations of this peptide in all 6 animals of control group. * $p < 0.05$.

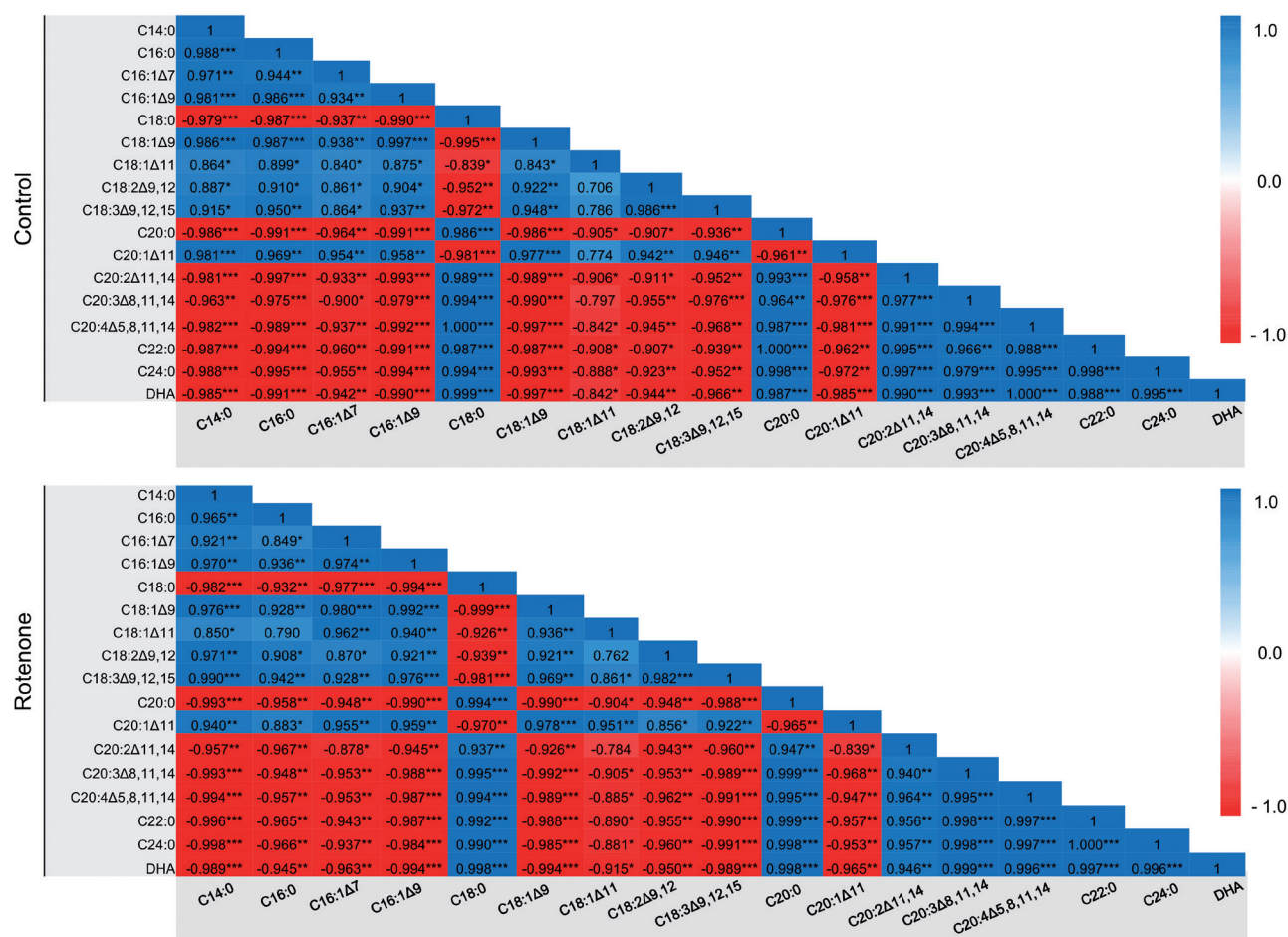


Figure 3. Associations among fatty acids identified in jejunum of control ($n = 6$) and rotenone-treated ($n = 6$) groups of animals in the study. Intensity of blue/red colour reflects strength of Pearson's coefficient. Positive correlation is expressed by blue shade, while red colour is relevant for negative manner of association between compared molecules. * $p < 0.05$, ** $p < 0.01$, *** $p < 0.001$.

analysis among individual values of all measured fatty acid intra-individually (Fig. 3).

Discussion

The results obtained from experimental work involving two types of toxic models of neurodegeneration provide a complex insight into changes occurring in esterified fatty acid composition in early stages of pathological process induced by rotenone treatment. Both experimental model systems share specific characteristics that could be considered common for both types of models. However, some of them are probably more specific for given experimental model. All presented changes in fatty acid composition were linked to parallel changes in α S concentration. Despite that we did not measure α S in present *in vitro* experiments, our previous study identified 10 μ M rotenone treatment for 24 h as an effective in stimulation of α S overexpression in SH-SY5Y cells. In addition, the fragmentation of microtubules, mainly composed by BIIIT, was confirmed as a rapid action associated with rotenone presence in the cell culture (Pokusa et al. 2021). In the case of mouse model, an increase in the expression of α S was identified in jejunum of several individuals after 14 weeks of rotenone treatment while in the case of control animals α S was under the detection limit of chosen ELISA test in all individuals (Fig. 1). Particularly, increased α S expression after rotenone treatment has been well documented in animal models involved in previous research works (Pan-Montojo et al. 2010; Giraldez-Perez et al. 2014). The elevation of α S is regarded as a hallmark of PD pathogenesis (Braak et al. 2003; Fanning et al. 2020). In pathological forms (oligomers and fibrils), α S is used for further propagation of PD-like pathogenesis in several types of models (Meredith et al. 2002; Fujita et al. 2006; Martin et al. 2006; Stichel et al. 2007; Varkey et al. 2010).

According to experimental research, α S is well documented to be closely associated with phospholipid bilayer in which it is anchored while its main function is probable to mediate the membrane dynamics (Amos et al. 2021). The natural form of α S is unfolded while the interaction of α S with lipid bilayer stabilizes α S in physiological (tetramer) form (Davidson et al. 1998). According to available data, fatty acids, which are predominantly considered to be beneficial for keeping α S in stabilized state are saturated. Among these, several experimental studies confirmed beneficial effects of C14:0 (MA), C16:0 (PA), C18:0 (SA), and C20:0 (AA) on pathological oligomeric α S levels (Sharon et al. 2003a; Lücke et al. 2006; Alecu and Bennett 2019; Tripathi et al. 2022). Regarding the group of saturated fatty acids detected in SH-SY5Y cells, our results obtained after 24 h treatment with 10 μ M rotenone confirmed the significant increase of SA, AA, and docosanoic acid. The tendency of an increase

was identified in MA and C24:0; however without statistical significance ($p = 0.14$ and 0.062 , respectively) (Table 1). Regarding saturated fatty acids, down-regulatory effect after 24 h of rotenone treatment was observed only in PA.

From the class of monounsaturated fatty acids, oleic acid is, according to the available literature, identified as risky in terms of possible α S accumulation and oligomerization (Fanning et al. 2019; Imberdis et al. 2019). Our experimental data revealed a decrease of oleic acid together with *cis*-vaccenic acid (C18:1 Δ^{11}). Similar effects as in the case of oleic acid were identified broadly in the class of PUFAs (Perrin et al. 2001). The only exception could be seen in the case of AA, which indeed led to the accumulation of oligomeric α S; however, this type of oligomers is easily degraded by proteasomes (Iljina et al. 2016; Xylaki et al. 2020). Our results obtained from cell culture experiments indicated the upregulation in case of eicosadienoic acid (C20:2 $\Delta^{11,14}$), docosadienoic acid (C22:2 $\Delta^{13,16}$), and γ -linolenic acid (C18:3 $\Delta^{6,9,12}$). We observed a numerical increase in AA levels but without statistical significance ($p = 0.112$).

According to these findings, we can summarize that in our experimental approach, the change in fatty acid composition is not associated with the degree of saturation but rather with the carbon chain length of fatty acids. Among 11 members of long-chain fatty acid group, we can see statistically significant decrease of 4 and increase of 3 fatty acids. Moreover, in the group of 4 detected very long-chain fatty acids, the increase was significantly confirmed in 2 of them. Importantly, Worth et al. (2014) demonstrated changes in pool of fatty acids activated by coenzyme A (CoA) in a study evaluating SH-SY5Y cells treated with rotenone of lower concentration (100 nM) for 6 hours. The authors detected a decrease in medium-chain saturated acyl-CoA species (C4–C14). Despite the neuronal origin of SH-SY5Y cells, these changes were described as a result of stimulated β -oxidation of medium-chain fatty acids to maintain the levels of acetyl-CoA in the cell. However, these results did not analyse changes in fatty acids esterified to cellular lipids of treated cells by rotenone. Therefore, our observations on fatty acid changes in lipids isolated from SH-SY5Y cells treated with rotenone can be considered as pioneering. We can conclude that behaviour of SH-SY5Y cells exposed to higher dose of rotenone (10 μ M) for longer period of time (24 h) exhibits different features when compared with Worth et al. (2014). In the future experiments, it would be hypothetically valuable to focus on the differences of β -oxidation occurring in peroxisomes and mitochondria. While the input for mitochondrial β -oxidative events is presented by long- and medium-chain fatty acids, the peroxisomes are exclusively aimed for shortening of very long-chain fatty acids with some minor capacities for long-chain fatty acids (Reddy and Hashimoto 2001). From this point of view, the mitochondrial toxin could operate also as a factor for asymmetrisation of

cellular β -oxidation processes. Beside the degradation, also *de novo* synthesis as well as fatty acid elongation could be involved in the hypothesis of future experiments aimed to elucidate the differences based on fatty acid length. While majority of long-chain fatty acid from C14 to C18 could be synthesized *de novo* in mitochondria, the origin of fatty acids from C20 length is a result of elongation processes mainly in endoplasmic reticulum (Jump 2009). In order to explain the specific impact of rotenone on fatty acid profile, it would be useful to investigate the specific role of other target(s) of rotenone in the cells. Several studies have already demonstrated a dose-dependent manner in micromolar range of rotenone effects on microtubule fragmentation as well as elevation of NADPH oxidase (NOX) activity (Zhou et al. 2012; Passmore et al. 2017). Both phenomena have been documented to be closely related to fatty acid metabolism in the cell. The fragmentation of microtubules stimulated by colchicine resulted in a significant decrease in the incorporation of palmitate and eicosa-8,11,14-trienoate into glycerolipids of Hep G2 human hepatoma cells (Marra and de Alaniz 2009). In addition, oleic acid treatment of SKOV-3 ovarian cancer cells significantly facilitated microtubule skeleton transformation during cell migration during which the microtubules were orientated towards the migration front (Masner et al. 2021). In the relevance with NOX, the potential regulatory effect of the enzyme on fatty acid metabolism needs to be investigated. However, the modulation of NOX activity by different fatty acids has been described. Oleic acid and other unsaturated fatty acids have modulatory effects on ROS production by NOX as well (Hatanaka et al. 2013). In 3T3-L1 adipocytes, excess of palmitate leads to stimulation of NOX activity while DHA has an opposite effect (Han et al. 2012). The release of AA from phospholipids by phospholipase A2 enzyme stimulates NOX activity (Rossary et al. 2007). The role of α S would represent a perspective aim of investigation in further research on fatty acid concentration through the regulation of phospholipases. Its direct inhibitory effect has been already observed in the case of phospholipase D2, which cleaves the headgroup of phosphatidylcholine to release choline and phosphatidic acid (Bendor et al. 2013).

According to previous studies of Pan-Montojo (2010), rotenone (in a dosage of 10 mg/kg) increased α S accumulation in the duodenum and ileum of mice. The accumulation of α S is considered as a risk factor and pre-stage of aggregation initiation in PD pathogenesis. The rotenone dosage in Pan-Montojo study (2010) was also able to accumulate α S in the neuronal ganglia after 3 months of daily oral treatment. Our results confirmed increased presence of α S also in jejunal part of GIT after equal time exposure to toxin. A significant increase was observed after 14 weeks of rotenone treatment in several individual animals while in the control group the presence of this protein did not reach the limit of detection using the selected ELISA method. Further investigation

of ER stress marker (GRP78) and neuronal marker BIIT exerted no significant change. Before measurement, we had hypothetically expected a decrease in BIIT values caused by degradation of the enteric nervous system as it was already observed in other cell line models (Ren et al. 2003). On the other hand, the increase in GRP78 was anticipated as a physiological reaction of the endoplasmic reticulum to the elevation of an unfolded protein relevant to the neurodegeneration process (Wang et al. 2009). The low statistical significance of changes between the control and experimental groups can be explained by a) the low ability of rotenone to induce relevant pathological changes in the jejunal part of the small intestine or b) by covering the relevant change by other non-sensitive cell types that represent the tissue of the gastrointestinal tract.

Similar as in SH-SY5Y cells, the composition of fatty acids, esterified to lipids in the tissue extract, was evaluated by GC chromatography. No significant changes in the concentration of fatty acids were observed. However, due to the large number of intra-individually obtained data, we were enabled to correlate this data with each other. As shown in Figure 2, the measured α S concentration in rotenone-treated mice strongly correlated with fatty acids according to its carbon chain length. While most long-chain fatty acids (C14–C18) correlated negatively with the level of α S, very long-chain fatty acids behaved in the opposite way. As an exception from overall tendency of C14–C18 fatty acids, stearic acid correlated in opposite manner than the rest of C14–C18 fatty acids. In the group of $C_{20} \leq$ fatty acids, gondoic acid ($C_{20:1\Delta^{11}}$) was the only one detected with positive correlation to α S. Both BIIT and GRP78 exert a moderate correlation with fatty acids after rotenone treatment. In both cases, the manner of correlation would be understood as opposite to that observed in α S. According to these findings, we can conclude that higher expression of α S is accompanied by higher representation of $C_{20} \leq$ fatty acids in cellular lipids. Whether this phenomenon is the result of increased α S expression or an adaptation mechanism of altered environment cannot be answered yet. According to several studies dealing with the effects of α S on lipid metabolism, abnormal α S metabolism is associated with prevalent accumulation of fatty acids with very long-chain fatty acids. This phenomenon is evident in animal models of peroxisomal dysfunction (Yakunin et al. 2010). The accumulation of very long-chain glycosphingolipids (GSLs) ($\geq C_{22}$) but not short-chain species induced α S pathology and neurological dysfunction. The selective reduction of long-chain GSLs ameliorated α S pathology through lysosomal cathepsins (Fredriksen et al. 2021). Similarly, as in the case of cell experiments, asymmetric division of correlation pattern of long-chain fatty acids is again a topic for discussion. However, for the hypothetical explanation, we can return to the phenomenon of *de novo* synthesis and elongation of long-chain fatty acid as well as

β -oxidation discussed previously. From the view of similarities in the metabolism of origination and degradation of C20 fatty acids to very long-chain fatty acids, it could be anticipated that their cellular concentrations could be more similar to these than to shorter members of long-chain fatty acids. Due to the lack of other relevant data, our results obtained in a toxic oral model of neurodegeneration could be evaluated as a pioneering finding in this field of research and strongly motivating to proceed the research in this direction. High potential can be seen especially in the possible relief of the pathological impact of aggregated α S forms, which could be achieved by modulating the fatty acid composition of biomembranes. In coherence with the theory about GIT origin of specific PD cases, an emphasis should be placed on the prevention of pathological α S conformation established by experimental approaches that focus on the modification of diet content, especially relevant fatty acids.

Animal welfare statement. The authors confirm that the ethical policies of the journal, as noted on the journal's author guidelines page, have been adhered to and the appropriate ethical review committee approval has been received. The authors confirm that they have followed EU standards for the protection of animals used for scientific purposes.

Conflict of interest. The authors declare no conflict of interest.

Acknowledgement. This study was supported by the Scientific Grant Agency of Ministry of Education of Slovak Republic under the contract No. VEGA 1/0299/20 and VEGA 2/0012/20.

References

- Alecu I, Bennett S (2019): Dysregulated lipid metabolism and its role in α -synucleinopathy in Parkinson's disease. *Front. Neurosci.* **13**, 328-350
<https://doi.org/10.3389/fnins.2019.00328>
- Alza NP, Iglesias González PA, Conde MA, Uranga RM, Salvador GA (2019): Lipids at the crossroad of α -synuclein function and dysfunction: biological and pathological implications. *Front. Cell. Neurosci.* **13**, 175-192
<https://doi.org/10.3389/fncel.2019.00175>
- Amos STA, Schwarz TC, Shi J, Cossins BP, Baker TS, Taylor RJ, Konrat R, Sansom MSP (2021): Membrane interactions of α -synuclein revealed by multiscale molecular dynamics simulations, Markov state models, and NMR. *J. Phys. Chem. B* **125**, 2929-2941
<https://doi.org/10.1021/acs.jpcc.1c01281>
- Assayag K, Yakunin E, Loeb V, Selkoe DJ, Sharon R (2007): Polyunsaturated fatty acids induce alpha-synuclein-related pathogenic changes in neuronal cells. *Am. J. Pathol.* **171**, 2000-2011
<https://doi.org/10.2353/ajpath.2007.070373>
- Bendor JT, Logan TP, Edwards RH (2013): The function of α -synuclein. *Neuron* **79**, 1044-1066
<https://doi.org/10.1016/j.neuron.2013.09.004>
- Bligh EG, Dyer WJ (1959): A rapid method of total lipid extraction and purification. *Can. J. Biochem. Physiol.* **37**, 911-917
<https://doi.org/10.1139/o59-099>
- Braak H, Del Tredici K, Rüb U, de Vos RA, Jansen Steur EN, Braak E (2003): Staging of brain pathology related to sporadic Parkinson's disease. *Neurobiol. Aging* **24**, 197-211
[https://doi.org/10.1016/S0197-4580\(02\)00065-9](https://doi.org/10.1016/S0197-4580(02)00065-9)
- Burré J, Sharma M, Südhof TC (2015): Definition of a molecular pathway mediating α -synuclein neurotoxicity. *J. Neurosci.* **35**, 5221-5232
<https://doi.org/10.1523/JNEUROSCI.4650-14.2015>
- Cannon JR, Tapias V, Na HM, Honick AS, Drolet RE, Greenamyre JT (2009): A highly reproducible rotenone model of Parkinson's disease. *Neurobiol. Dis.* **34**, 279-290
<https://doi.org/10.1016/j.nbd.2009.01.016>
- Davidson WS, Jonas A, Clayton DF, George JM (1998): Stabilization of alpha-synuclein secondary structure upon binding to synthetic membranes. *J. Biol. Chem.* **273**, 9443-9449
<https://doi.org/10.1074/jbc.273.16.9443>
- Fahn S, Sulzer D (2004): Neurodegeneration and neuroprotection in Parkinson disease. *NeuroRx* **1**, 139-154
<https://doi.org/10.1602/neurorx.1.1.139>
- Fanning S, Haque A, Imberdis T, Baru V, Barrasa MI, Nuber S, Termine D, Ramalingam N, Ho G, Noble T, et al. (2019): Lipidomic analysis of α -synuclein neurotoxicity identifies stearoyl CoA desaturase as a target for Parkinson treatment. *Mol. Cell.* **73**, 1001-1014
<https://doi.org/10.1016/j.molcel.2018.11.028>
- Fanning S, Selkoe D, Dettmer U (2020): Parkinson's disease: proteinopathy or lipidopathy? *NPJ Parkinsons Dis.* **6**, 3-19
<https://doi.org/10.1038/s41531-019-0103-7>
- Fecchio C, Palazzi L, de Laureto PP (2018): α -Synuclein and polyunsaturated fatty acids: molecular basis of the interaction and implication in neurodegeneration. *Molecules* **23**, 1531-1551
<https://doi.org/10.3390/molecules23071531>
- Fredriksen K, Aivazidis S, Sharma K, Burbidge KJ, Pitcairn C, Zunke F, Gelyana E, Mazzulli JR (2021): Pathological α -syn aggregation is mediated by glycosphingolipid chain length and the physiological state of α -syn in vivo. *Proc. Natl. Acad. Sci. USA* **118**, e2108489118-e2108489130
<https://doi.org/10.1073/pnas.2108489118>
- Fujita Y, Ohama E, Takatama M, Al-Sarraj S, Okamoto K (2006): Fragmentation of Golgi apparatus of nigral neurons with alpha-synuclein-positive inclusions in patients with Parkinson's disease. *Acta Neuropathol.* **112**, 261-265
<https://doi.org/10.1007/s00401-006-0114-4>
- Gai WP, Yuan HX, Li XQ, Power JT, Blumbergs PC, Jensen PH (2000): In situ and in vitro study of colocalization and segregation of alpha-synuclein, ubiquitin, and lipids in Lewy bodies. *Exp. Neurol.* **166**, 324-333
<https://doi.org/10.1006/exnr.2000.7527>
- Galvagnion C, Buell AK, Meisl G, Michaels TC, Vendruscolo M, Knowles TP, Dobson CM (2015): Lipid vesicles trigger α -synuclein aggregation by stimulating primary nucleation. *Nat. Chem. Biol.* **11**, 229-234
<https://doi.org/10.1038/nchembio.1750>
- Garaiova M, Mietkiewska E, Weselake RJ, Holic R (2017): Metabolic engineering of *Schizosaccharomyces pombe* to produce puniic

- acid, a conjugated fatty acid with nutraceutical properties. *Appl. Microbiol. Biotechnol.* **101**, 7913-7922
<https://doi.org/10.1007/s00253-017-8498-8>
- Giráldez-Pérez R, Antolín-Vallespín M, Muñoz M, Sánchez-Capelo A (2014): Models of α -synuclein aggregation in Parkinson's disease. *Acta Neuropathol. Commun.* **2**, 176-193
<https://doi.org/10.1186/s40478-014-0176-9>
- Han CHJ, Umamoto T, Omer M, Den Hartigh LJ, Chiba T, LeBoeuf R, Buller CL, Sweet IR, Pennathur S, Abel ED, Chait A (2012): NADPH oxidase-derived reactive oxygen species increases expression of monocyte chemotactic factor genes in cultured adipocytes. *J. Biol. Chem.* **287**, 10379-10393
<https://doi.org/10.1074/jbc.M111.304998>
- Hatanaka E, Dermargos A, Hirata AE, Vinolo MAR, Carpinelli AR, Newsholme P, Armelin HA, Curi R (2013): Oleic, linoleic and linolenic acids increase ROS production by fibroblasts via NADPH oxidase activation. *PLoS One* **8**, e58626-e58634
<https://doi.org/10.1371/journal.pone.0058626>
- Ilijina M, Tosatto L, Choi ML, Sang JC, Ye Y, Hughes CD, Bryant CE, Gandhi S, Klenerman D (2016): Arachidonic acid mediates the formation of abundant α -helical multimers of α -synuclein. *Sci. Rep.* **6**, 33928-33942
<https://doi.org/10.1038/srep33928>
- Imberdis T, Negri J, Ramalingam N, Terry-Kantor E, Ho G, Fanning S, Stirtz G, Kim TE, Levy OA, Young-Pearse TL, et al. (2019): Cell models of lipid-rich α -synuclein aggregation validate known modifiers of α -synuclein biology and identify stearyl-CoA desaturase. *Proc. Natl. Acad. Sci. USA* **116**, 20760-20769
<https://doi.org/10.1073/pnas.1903216116>
- Inden M, Kitamura Y, Abe M, Tamaki A, Takata K, Taniguchi T (2011): Parkinsonian rotenone mouse model: reevaluation of long-term administration of rotenone in C57BL/6 mice. *Biol. Pharm. Bull.* **34**, 92-96
<https://doi.org/10.1248/bpb.34.92>
- Innos J, Hickey MA (2021): Using rotenone to model Parkinson's disease in mice: A review of the role of pharmacokinetics. *Chem. Res. Toxicol.* **34**, 1223-1239
<https://doi.org/10.1021/acs.chemrestox.0c00522>
- Jump DB (2009): Mammalian fatty acid elongases. *Methods. Mol. Biol.* **579**, 375-389
https://doi.org/10.1007/978-1-60761-322-0_19
- Lücke C, Gantz DL, Klimtchuk E, Hamilton JA (2006): Interactions between fatty acids and α -synuclein. *J. Lipid. Res.* **47**, 1714-1724
<https://doi.org/10.1194/jlr.M600003-JLR200>
- Manna M, Murarka RK (2021): Polyunsaturated fatty acid modulates membrane-bound monomeric α -synuclein by modulating membrane microenvironment through preferential interactions. *ACS Chem. Neurosci.* **12**, 675-688
<https://doi.org/10.1021/acchemneuro.0c00694>
- Marra CA, de Alaniz MJ (2009): Microtubule depolymerization modifies the incorporation of fatty acids into glycerolipids. *Med. Sci. Monit.* **15**, BR157-BR165
- Martin LJ, Pan Y, Price AC, Sterling W, Copeland NG, Jenkins NA, Price DL, Lee MK (2006): Parkinson's disease α -synuclein transgenic mice develop neuronal mitochondrial degeneration and cell death. *J. Neurosci.* **26**, 41-50
<https://doi.org/10.1523/JNEUROSCI.4308-05.2006>
- Masner M, Lujea N, Bisbal M, Acosta C, Kunda P (2021): Linoleic and oleic acids enhance cell migration by altering the dynamics of microtubules and the remodeling of the actin cytoskeleton at the leading edge. *Sci. Rep.* **11**, 14984 - 15001
<https://doi.org/10.1038/s41598-021-94399-8>
- Meredith GE, Totterdell S, Petroske E, Santa Cruz K, Callison RC Jr, Lau YS (2002): Lysosomal malfunction accompanies α -synuclein aggregation in a progressive mouse model of Parkinson's disease. *Brain Res.* **956**, 156-165
[https://doi.org/10.1016/S0006-8993\(02\)03514-X](https://doi.org/10.1016/S0006-8993(02)03514-X)
- Panicker N, Ge P, Dawson VL, Dawson TM (2021): The cell biology of Parkinson's disease. *J. Cell. Biol.* **220**, e202012095-e202012126
<https://doi.org/10.1083/jcb.202012095>
- Pan-Montojo F, Anichtchik O, Dening Y, Knels L, Pursche S, Jung R, Jackson S, Gille G, Spillantini MG, Reichmann H, Funk RHW (2010): Progression of Parkinson's disease pathology is reproduced by intragastric administration of rotenone in mice. *PLoS One* **5**, e8762-e8772
<https://doi.org/10.1371/journal.pone.0008762>
- Passmore JB, Pinho S, Gomez-Lazaro M, Schrader M (2017): The respiratory chain inhibitor rotenone affects peroxisomal dynamics via its microtubule-destabilising activity. *Histochem. Cell. Biol.* **148**, 331-341
<https://doi.org/10.1007/s00418-017-1577-1>
- Perrin RJ, Woods WS, Clayton DF, George JM (2001): Exposure to long chain polyunsaturated fatty acids triggers rapid multimerization of synucleins. *J. Biol. Chem.* **276**, 41958-41962
<https://doi.org/10.1074/jbc.M105022200>
- Pokusa M, Hajdúchová D, Menichová V, Evinová A, Hatoková Z, Kráľová-Trančíková A (2021): Vulnerability of subcellular structures to pathogenesis induced by rotenone in SH-SY5Y cells. *Physiol. Res.* **70**, 89-99
<https://doi.org/10.33549/physiolres.934477>
- Ramakrishnan M, Jensen PH, Marsh D (2003): α -Synuclein association with phosphatidylglycerol probed by lipid spin labels. *Biochem.* **42**, 12919-12926
<https://doi.org/10.1021/bi035048e>
- Reddy JK, Hashimoto T (2001): Peroxisomal beta-oxidation and peroxisome proliferator-activated receptor α : an adaptive metabolic system. *Annu. Rev. Nutr.* **21**, 193-230
<https://doi.org/10.1146/annurev.nutr.21.1.193>
- Ren Y, Zhao J, Feng J (2003) Parkin binds to α / β tubulin and increases their ubiquitination and degradation. *J. Neurosci.* **23**, 3316-3324
<https://doi.org/10.1523/JNEUROSCI.23-08-03316.2003>
- Rossary A, Arab K, Goudable J, Steghens JP (2007) Régulation de l'activité des NADPH oxydases en présence d'acides gras (Fatty acids regulate NOX activity). *Ann. Biol. Clin. (Paris)*. **65**, 33-40 (in French)
- Schommer J, Marwarha G, Nagamoto-Combs K, Ghribi O (2018): Palmitic acid-enriched diet increases α -synuclein and tyrosine hydroxylase expression levels in the mouse brain. *Front. Neurosci.* **12**, 552-565
<https://doi.org/10.3389/fnins.2018.00552>
- Shah A, Han P, Wong MY, Chang RC, Legido-Quigley C (2019): Palmitate and stearate are increased in the plasma in a 6-OHDA model of Parkinson's disease. *Metabolites* **9**, 31-45

- <https://doi.org/10.3390/metabo9020031>
- Sharon R, Bar-Joseph I, Frosch MP, Walsh DM, Hamilton JA, Selkoe DJ (2003a): The formation of highly soluble oligomers of alpha-synuclein is regulated by fatty acids and enhanced in Parkinson's disease. *Neuron* **37**, 583-595
[https://doi.org/10.1016/S0896-6273\(03\)00024-2](https://doi.org/10.1016/S0896-6273(03)00024-2)
- Sharon R, Bar-Joseph I, Mirick GE, Serhan CN, Selkoe DJ (2003b): Altered fatty acid composition of dopaminergic neurons expressing alpha-synuclein and human brains with alpha-synucleinopathies. *J. Biol. Chem.* **278**, 49874-49881
<https://doi.org/10.1074/jbc.M309127200>
- Shimohama S, Sawada H, Kitamura Y, Taniguchi T (2003): Disease model: Parkinson's disease. *Trends Mol. Med.* **9**, 360-365
[https://doi.org/10.1016/S1471-4914\(03\)00117-5](https://doi.org/10.1016/S1471-4914(03)00117-5)
- Stichel CC, Zhu XR, Bader V, Linnartz B, Schmidt S, Lübbert H (2007): Mono- and double-mutant mouse models of Parkinson's disease display severe mitochondrial damage. *Hum. Mol. Genet.* **16**, 2377-2393
<https://doi.org/10.1093/hmg/ddm083>
- Tasselli M, Chaumette T, Paillusson S, Monnet Y, Lafoux A, Huchet-Cadiou C, Aubert P, Hunot S, Derkinderen P, Neunlist M (2013): Effects of oral administration of rotenone on gastrointestinal functions in mice. *Neurogastroenterol. Motil.* **25**, e183-93
<https://doi.org/10.1111/nmo.12070>
- Tripathi A, Alnakhala H, Terry-Kantor E, Newman A, Liu L, Imberdis T, Fanning S, Nuber S, Ramalingam N, Selkoe D, Dettmer U (2022): Pathogenic mechanisms of cytosolic and membrane-enriched alpha-synuclein converge on fatty acid homeostasis. *J. Neurosci.* **42**, 2116-2130
<https://doi.org/10.1523/JNEUROSCI.1881-21.2022>
- Varkey J, Isas JM, Mizuno N, Jensen MB, Bhatia VK, Jao CC, Petrlova J, Voss JC, Stamou DG, Steven AC, Langen R (2010): Membrane curvature induction and tubulation are common features of synucleins and apolipoproteins. *J. Biol. Chem.* **285**, 32486-32493
<https://doi.org/10.1074/jbc.M110.139576>
- Vincent BM, Tardiff DF, Piotrowski JS, Aron R, Lucas MC, Chung CY, Bacherman H, Chen Y, Pires M, Subramaniam R, et al. (2018): Inhibiting stearoyl-CoA desaturase ameliorates alpha-synuclein cytotoxicity. *Cell. Rep.* **25**, 2742-2754
<https://doi.org/10.1016/j.celrep.2018.11.028>
- Wang J, Hoekstra JG, Zuo C, Cook TJ, Zhang J (2013): Biomarkers of Parkinson's disease: current status and future perspectives. *Drug Discov. Today* **18**, 155-162
<https://doi.org/10.1016/j.drudis.2012.09.001>
- Wang M, Wey S, Zhang Y, Ye R, Lee AS (2009): Role of the unfolded protein response regulator GRP78/BiP in development, cancer, and neurological disorders. *Antioxid. Redox. Signal.* **11**, 2307-2316
<https://doi.org/10.1089/ars.2009.2485>
- Worth AJ, Basu SS, Snyder NW, Mesaros C, Blair IA (2014): Inhibition of neuronal cell mitochondrial complex I with rotenone increases lipid beta-oxidation, supporting acetyl-Coenzyme A levels. *J. Biol. Chem.* **289**, 26895-26903
<https://doi.org/10.1074/jbc.M114.591354>
- Xia R, Mao ZH (2012): Progression of motor symptoms in Parkinson's disease. *Neurosci. Bull.* **28**, 39-48
<https://doi.org/10.1007/s12264-012-1050-z>
- Xiong N, Huang J, Zhang Z, Zhang Z, Xiong J, Liu X, Jia M, Wang F, Chen C, Cao X, et al. (2009): Stereotaxical infusion of rotenone: a reliable rodent model for Parkinson's disease. *PLoS One* **4**, e7878.
<https://doi.org/10.1371/journal.pone.0007878>
- Xylaki M, Boumpourea I, Kokotou MG, Marras T, Papadimitriou G, Kloukina I, Magrioti V, Kokotos G, Vekrellis K, Emmanouilidou E (2020): Changes in the cellular fatty acid profile drive the proteasomal degradation of alpha-synuclein and enhance neuronal survival. *FASEB J.* **34**, 15123-15145
<https://doi.org/10.1096/fj.202001344R>
- Yakunin E, Loeb V, Kisos H, Biala Y, Yehuda S, Yaari Y, Selkoe DJ, Sharon R (2012): A-synuclein neuropathology is controlled by nuclear hormone receptors and enhanced by docosahexaenoic acid in a mouse model for Parkinson's disease. *Brain. Pathol.* **22**, 280-294
<https://doi.org/10.1111/j.1750-3639.2011.00530.x>
- Yakunin E, Moser A, Loeb V, Saada A, Faust P, Crane DI, Baes M, Sharon R (2010): Alpha-synuclein abnormalities in mouse models of peroxisome biogenesis disorders. *J. Neurosci. Res.* **88**, 866-876
<https://doi.org/10.1002/jnr.22246>
- Zhou H, Zhang F, Chen SH, Zhang D, Wilson B, Hong JS, Gao HM (2012): Rotenone activates phagocyte NADPH oxidase by binding to its membrane subunit gp91phox. *Free. Radic. Biol. Med.* **52**, 303-313
<https://doi.org/10.1016/j.freeradbiomed.2011.10.488>

Received: August 5, 2022

Final version accepted: September 23, 2022